



Preparation of modified ZnO nanoparticles for photocatalytic degradation of chlorobenzene

Pallavi Nagaraju¹ · Shivaraju Harikaranahalli Puttaiah^{1,2} · Kitirote Wantala³ · Behzad Shahmoradi^{2,4}

Received: 24 March 2020 / Accepted: 6 May 2020 / Published online: 18 May 2020
© The Author(s) 2020

Abstract

Volatile organic compounds (VOCs) are one of the major pollutants present in the petrochemical industrial effluents. These VOCs have high vapor pressure, which makes it to be dispersed into the atmosphere easily. Chlorobenzene is one such VOC, which has an ability to cause adverse impacts on human health by damaging the central nervous systems. The available treatment methods are unable to effectively treat such VOCs in environment. Photocatalytic degradation is the effective and economical methods, which are being used for the treatment of such pollutants. ZnO is one of the widely accepted photocatalyst, but it has a limitation of wide band-gap energy utilization. This paper mainly investigates the preparation of metal-doped ZnO nanoparticles using solgel technique and its application for the degradation of chlorobenzene in an aqueous media under different light sources. Among the modified ZnO nanoparticles prepared (Ag/ZnO, Cd/ZnO and Pb/ZnO), Pb/ZnO was found to be very effective in the degradation of chlorobenzene and achieved up to 100% within a short duration (< 120 min). The Pb/ZnO was also used as a photocatalyst in a vertical continuous photoreactor for the photodegradation of chlorobenzene using LED light.

Keywords Volatile organic compound · Chlorobenzene · Nanoparticles · Photocatalysis, modified ZnO

Introduction

Volatile organic compounds (VOCs) are the organic compounds, which have high vapor pressure at room temperature, and they are characterized by low water solubility (Goldstein Allen 2007; Guo et al. 2009). Rapid industrialization and urbanization have led to serious environmental pollution problems that impact on the human health at global level. VOCs play a critical role in photochemical reactions, which give rise to highly toxic secondary and intermediate

pollutants. However, severe impacts of VOCs which are disposed by anthropogenic activities, on the human health and environment from the past few years, have been realized (Tanizaki et al. 2007). Recently, evidences are rapidly growing to show the potential health hazards associated with VOCs and their involvement with global climate change and few VOCs species were shown to be highly toxic, mutagenic and carcinogenic (Said Ismail and Hameed 2013). Apart from potential health impacts of VOCs, they are also involved in photochemical reactions leading to the formation of oxidants, which have serious deleterious effects on human health, agricultural crops, trees, natural vegetation, buildings, materials, etc. (Lin et al. 2013; Prabhat Kumar et al. 2011; Zou et al. 2006). Chlorobenzene is a colorless and flammable aromatic compound with molecular formula C_6H_5Cl . Chlorobenzene is primarily used as a solvent, a degreasing agent and as a chemical intermediate in various industries. Chlorobenzene causes various health effects like skin irritation, skin and eyes allergies, nose and throat rashes, and exposure to very high concentration can cause headache, dizziness. Acute inhalation causes narcosis, restlessness, tremors and muscle spasms. Chronic (long-term) exposure of humans to chlorobenzene affects the central

✉ Shivaraju Harikaranahalli Puttaiah
shivarajuenvi@gmail.com

¹ Department of Water and Health, JSS Academy of Higher Education and Research, Mysuru 570015, India

² Center for Water, Food and Energy, GREENS Trust, Harikaranahalli Village, Dombarnahalli Post, Turuvekere Taluka, Tumkur District, Karnataka 572215, India

³ Department of Chemical Engineering, Faculty of Engineering, Khon Kaen University, Khon Kaen, Thailand

⁴ Department of Environmental Health Engineering, Environmental Health Research Center, Kurdistan University of Medical Sciences, Sanandaj, Iran

nervous system (CNS). They can damage the lung, liver and kidney by inhalation. Signs of neurotoxicity in humans include numbness, cyanosis, hyperesthesia (increased sensation) and muscle spasms. EPA has classified chlorobenzene as a Group D, not classifiable as to human carcinogenicity. There are various technologies, which have been currently used for the treatment or elimination of VOCs. Physicochemical and biological treatment methods are available for the removal of VOCs by recovery method or destruction method (Berenjian et al. 2012; Das et al. 2004; Font et al. 2011; Huang et al. 2016; Prabhat Kumar et al. 2011; Reddy et al. 2011). Biological treatment techniques are designed on the capability of microorganisms to degrade the organic pollutants under aerobic conditions through oxidative and reductive reactions to water vapor, carbon dioxide, inorganic products and organic biomass. The biological techniques confide on two important fundamental mechanisms. Drawback with absorption technique generates wastewater which needs further treatment, high initial investment, difficult in design, start-up time constraints, requires a precise maintenance of the system, and is not suitable method for lower concentrations of VOCs (Khan and Kr. Ghoshal 2000; Prabhat Kumar et al. 2011). The traditional methods used for VOCs treatment such as adsorption on activated charcoal, biofiltration and normal treatment methods are challenged by many factors such as energy requirements, expenses for scaling up large-scale applications, inefficient to degrade most of these organic compounds, generation of toxic organic by-products, reusability problem, generation of waste and waste disposal problem (Eltouny 2009; Huang et al. 2016). Advanced oxidation process (AOP) is a process that associates the production of reactive oxidizing agent such as hydroxyl radicals in sufficient quantity for the degradation of complex organic compounds present in both water and wastewater. The preeminent objective of AOP is to completely degrade the toxic organic pollutants to non-detectable limits from the ppb or ppm range without generating hazardous secondary pollutants.

Photocatalysis can use a renewable energy source widely in the treatment of pollutants; thereby, it is environmentally friendly and economic (Ameta et al. 2012). Photocatalysis using semiconductor has been enormously demonstrated for environmental applications as a cleanup process. Photocatalysis pathway is considered to be following a green chemistry due to its environmental friendly approach in degradation of various organic pollutants. Heterogeneous photocatalysis has been extensively used for the wastewater treatment and pollutant degradation into environmental friendly compounds. Research has been carried out to use zinc oxide (ZnO) as a photocatalyst for the degradation of various hazardous industrial dyes and organic contaminants in water and wastewater. ZnO is one of the remarkable semiconductor-based photocatalytic material, and it has been

widely used in various applications such as optical, electronics, optoelectronics, catalytic and lasers. The scope of the present research is to investigate the photocatalytic degradation of chlorobenzene using modified ZnO nanoparticles in a batch reactor under different light sources and to find an economical way to treat volatile organic compound.

Material and methodology

ZnO has great beneficial properties for photodegradation of various organic contaminants, visible light-based photocatalysis attributed to the wide band-gap energy (3.37 eV) and large free-excitation binding energy (60 meV) (Malik et al. 2013; Meena and Chouhan 2015; Rangkooy et al. 2012). Properties such as physicochemical stability, high thermal conductivity, high electron mobility, nontoxicity and large binding energy have made it as a novel semiconductor in the field of photocatalytic applications (Brintha and Ajitha 2015; Chen and Mao 2007; Hasnidawani et al. 2016; Khan et al. 2014). Nowadays, TiO_2 has been widely used semiconductor in photocatalytic applications (Crutzen et al. 1999; Malekshahi Byranvand et al. 2013; Aneesh and Vanaja 2007; Rajput 2015; Salahuddin et al. 2015; Tseng et al. 2010; Wong et al. 2011) and modified ZnO can be an appropriate alternative semiconductor in photocatalytic applications, since it has showed a wider range of band-gap energy and photocatalytic activities significantly under visible range of photon sources (Ameta et al. 2012; Prieto et al. 2007; Zou et al. 2004). However, controlling the surface redox reactions and postponing the recombination of photoinduced electron-hole pairs and band-gap tuning are the major challenges that need to be addressed to enhance overall photocatalytic degradation efficiency of ZnO (Bacaksiz et al. 2008; Chen et al. 2003; Kim and Choi 2007; Sharma et al. 2014). The modification of ZnO semiconductor with noble metals and nonmetals has significantly attracted attention in semiconductor based heterogeneous photocatalysis (Anandan et al. 2010; Djurišić et al. 2014; Nakata and Fujishima 2012; Ramesh 2013; Rehman et al. 2009; Sharma et al. 2014). Recently, various metal and nonmetal ions such as Ag, Cd, Fe, Mn, Co, Ni, Mg, and Cu have been used as doping ions to reduce the recombination of electron-hole pairs and reduce band-gap energy (Anandan et al. 2010; Djurišić et al. 2014; Nakata and Fujishima 2012; Ramesh 2013; Rehman et al. 2009; Sharma et al. 2014; Zaleska-medynska 2006).

Preparation and characterization of modified ZnO nanoparticles

Preparation of modified ZnO nanoparticles such as Ag-doped ZnO (Ag/ZnO), Cd-doped ZnO (Cd/ZnO) and

Pb-doped ZnO (Pb/ZnO) was carried out using solgel technique under alkaline conditions. Silver nitrite, cadmium sulfate and lead acetate were used as the dopant sources for the preparation of Ag (1%)-, Cd (1%)- and Pb (1%)-doped ZnO nanoparticles, respectively, with reagent grade ZnO powder as a core precursor of ZnO. Standard solgel procedures were used for the preparation of modified ZnO nanoparticles (Midhun et al. 2017; Shivaraju 2012; Shivaraju and Byrappa 2012; Shivaraju and Chandrashekar 2012; Shivaraju et al. 2016). The obtained final products were dried at room temperature and calcinated at 500 °C for 2-h duration using preheated muffle furnace. As-prepared modified ZnO nanoparticles were characterized for band-gap energy using UV–Vis spectrophotometer (Shimazu UV-1800), powder X-ray diffraction (Bruker-Microstar Proteum 8), scanning electron microscopic images with energy-dispersive X-ray analysis (EVO LS 15, Carl Zeiss, Germany), Fourier transformed infrared spectroscopy (Shimadzu IRAffinity-1S), dynamic light scattering (Malvern Instruments Ltd.), BET surface area (Micromeritics TRIstar 3020, USA) and photocatalytic activities. The modified ZnO nanoparticles were used for the degradation of chlorobenzene of known concentration for duration of 5 h in a batch reactor. The initial and final concentration of chlorobenzene was determined using GC coupled with mass spectrometer (Shimadzu, Tokyo, Japan).

Photocatalytic degradation of chlorobenzene using model vertical continuous photo reactor

Based on the results obtained during photocatalytic degradation of chlorobenzene, a potential real-time application of semiconductor-based nanophotocatalyst in a laboratory-scale continuous reactor model was fabricated and demonstrated using aqueous solution. Designing of continuous photoreactor was carried out for vertical models by considering the flow rate, light illumination and catalyst loading mode. Reaction vessels made with quartz materials were used with less energy consuming photon sources such as light-emitting diodes (LEDs). Photocatalytic degradation of chlorobenzene was carried out using batch scale photoreactor of 50 mL capacity in a closed system under different light sources. Aqueous solution of about 20 µg/L of chlorobenzene was used for photocatalytic studies with 2 h irradiation time. About 25 mg of each modified ZnO nanoparticles (Ag/ZnO, Cd/ZnO and Pb/ZnO) was dispersed in aqueous solution of chlorobenzene and irradiated to different light sources (fluorescent light, UV light, tungsten light and LED light). Initial and final concentration of chlorobenzene in aqueous media was measured by dynamic liquid phase microextraction method (Castellote and Bengtsson 2011) using QP5000 GC–MS instrument (Shimadzu, Tokyo, Japan) equipped with fused-silica capillary column

(30 m × 0.32 mm × 0.25 µm) coated with bonded film of DB-1/5MS.

Results and discussions

As-prepared modified ZnO nanoparticles were characterized, and photocatalytic degradation using model dye solution under different light sources was studied. The photocatalytic activity of the modified ZnO for the degradation of chlorobenzene was also carried out in a laboratory-scale batch photoreactor under different light sources.

Characterization of modified ZnO nanoparticles

Band-gap energy

Band-gap energy (optical absorption properties) of pure ZnO and modified ZnO nanoparticles such as Ag/ZnO, Cd/ZnO and Pb/ZnO was studied using UV–Vis spectroscopic methods, and the results obtained can be seen in Fig. 1. It was noticed that the optical absorption edges of modified ZnO nanoparticles were considerably shifted toward the wavelength of visible range when compared to pure ZnO. The equation $E_g = 1239.8/\lambda$ was used to calculate the band-gap energy of all modified ZnO nanoparticles, where E_g is the band gap (eV) and λ is the wavelength of the absorption edges in the UV–Vis spectrum (Zaleska-medynska 2006). Band-gap energy was observed to 3.15, 2.97, 2.91 and 2.81 eV for pure ZnO, Ag/ZnO, Cd/ZnO and Pb/ZnO nanoparticles, respectively. Highest band-gap energy shifting toward the visible range was observed in Pb/ZnO than Cd/ZnO and Pb/ZnO. These results indicated that the presence of Pb, Cd and Ag in ZnO system considerably reduces the

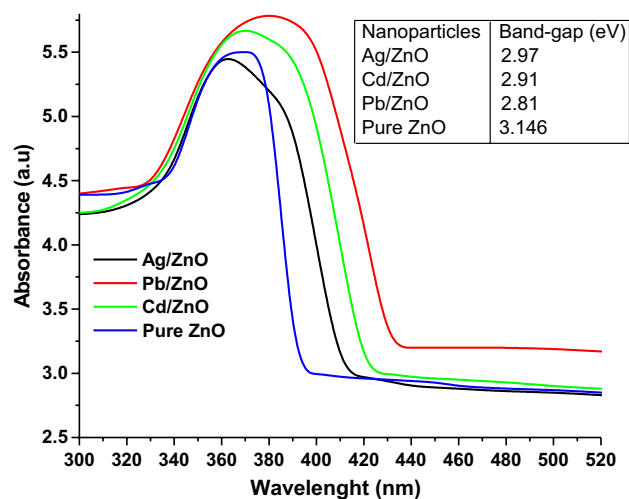


Fig. 1 Absorption edges and band-gap energies of modified ZnO nanoparticles in the UV–Vis spectrum

band-gap energy up to 10.7%, 7.5% and 5.6% toward visible range. It is worthy to note that absorption intensity was high for Pb/ZnO compared to pure ZnO indicating the potential photocatalytic activity in the wavelength of visible range.

Powder X-ray diffraction

Crystalline structure and phase identification of modified ZnO (Ag-, Cd-, Pb-doped ZnO) nanoparticles were investigated using powder X-ray diffraction technique with CuK α ($\lambda = 1.54056$ Å) as source with scanning range 10–80° (2 θ). The crystalline phases of modified ZnO nanoparticles were identified by comparing with JCPDS files (PCPDF WIN-2.01). Average crystallite sizes were estimated from the Debye–Scherrer's equation $D = k\lambda/\beta\cos\theta$, where 'D' is the crystallite size; 'k' is a constant (= 0.9 assuming that the particles are spherical); ' λ ' is the wavelength of the X-rays; ' β ' is the FWHM; ' θ ' is the diffraction angle in radians. Figure 2 shows the powder X-ray diffraction patterns of modified ZnO nanoparticles. XRD patterns of all modified ZnO nanoparticles showed sharp and high-intensity peaks when

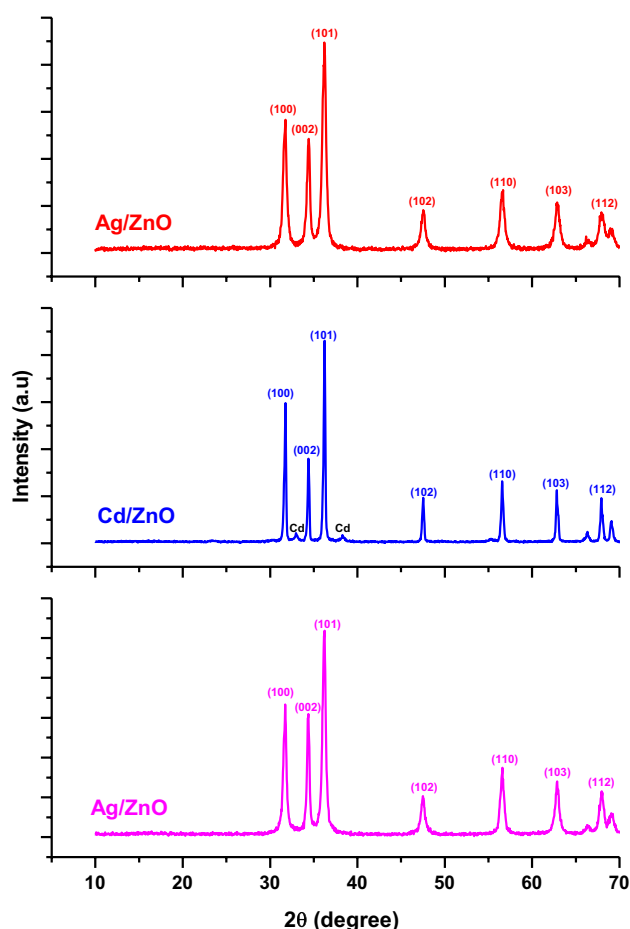


Fig. 2 Powder X-ray diffraction patterns of modified ZnO nanoparticles

compared to pure ZnO (undoped) that may be attributed to the influence of dopants and solgel conditions under alkaline environment. The results obtained indicated highly crystalline phase of modified ZnO nanoparticles and XRD patterns were well matched with PCPDF: 050664. A strong peak (101) of ZnO was observed at $2\theta = 36.24^\circ$. Powder XRD patterns of modified ZnO nanoparticles showed all strong peaks corresponding to known diffraction maxima of ZnO ($2\theta = 31.7^\circ, 34.4^\circ, 36.2^\circ, 56.6^\circ$ and 62.8°). The average crystalline sizes of modified ZnO nanoparticles were estimated using FWHM of the diffraction peak of XRD (Table 1).

Scanning electron microscopy with energy-dispersive X-ray analysis

Surface morphology and elemental analysis of modified ZnO nanoparticles were studied by scanning electron microscopy with energy-dispersive X-ray analysis. SEM images of Ag/ZnO and Cd/ZnO nanoparticles were observed to be irregular in shape and aggregated. Energy-dispersive X-ray analysis of Ag/ZnO (Fig. 3) and Cd/ZnO (Fig. 4) nanoparticles showed the presence of Ag and Cd elements in ZnO crystalline system, respectively. Ag/ZnO and Cd/ZnO nanoparticles were observed to be poly-scale in nature and agglomerated. When Pb/ZnO nanoparticles were observed under scanning electron microscopy, nanorod shaped morphology with well-crystalline structure and uniform-sized nanoparticles were observed (Fig. 5). The diameter of Pb/ZnO nanorods was observed approximately 60 to 150 nm range, and it was also confirmed by XRD as well as DLS characterization results. Well-crystalline phase of modified ZnO particles was apparently stable from the perspective of chemical reactions that enhances the photocatalytic activities of Pb/ZnO.

Fourier transformed infrared spectroscopy

The functional groups and structural elucidations of modified ZnO nanoparticles were carried out using FTIR method. FTIR spectra of pure ZnO and modified ZnO nanoparticles can be seen in Fig. 6. The stretching bands corresponding to ZnO were obtained in the range of 500 to 400 cm^{-1} in all the FTIR spectra. The band at 1430 cm^{-1} corresponding to C=O modes of vibration was observed in all FTIR spectra.

Table 1 Average crystalline size of modified ZnO nanoparticles

Modified ZnO nanoparticles	FWHM	Average crystalline sizes (nm)
Ag/ZnO	0.045	191.8
Cd/ZnO	0.031	287.7
Pb/ZnO	0.120	71.9

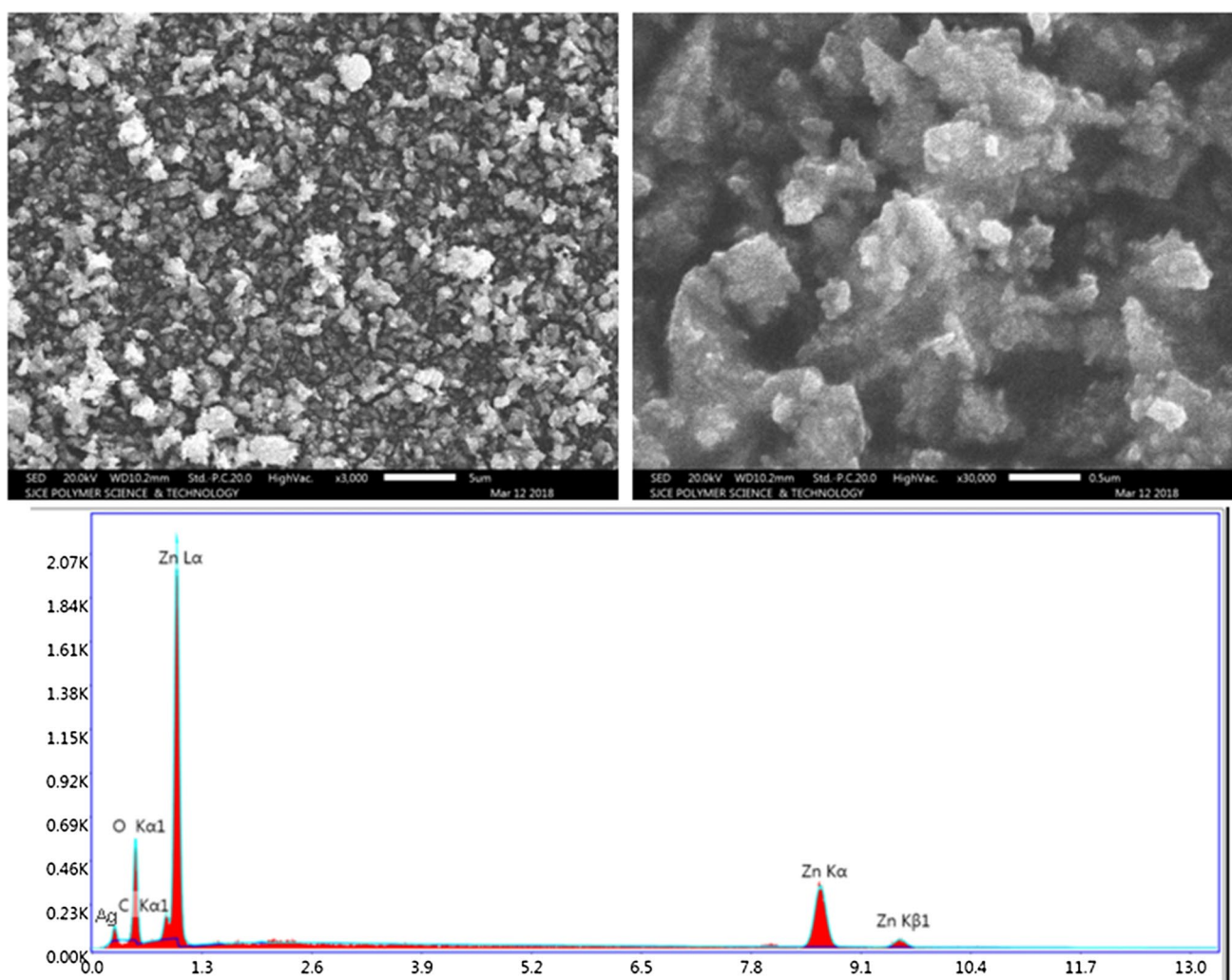


Fig. 3 Scanning electron microscopic images with energy-dispersive X-ray analysis of Ag/ZnO nanoparticles

The broad absorption peaks in the range of $3200\text{--}3600\text{ cm}^{-1}$ corresponding to O–H group of H_2O were observed in modified ZnO nanoparticles, and the existence of moistures on the surface of all modified ZnO nanoparticles was indicated. FTIR spectrum of Ag/ZnO and Cd/ZnO nanoparticles showed broad stretching vibration bands at $900\text{--}1150\text{ cm}^{-1}$ corresponding to Zn–O–Ag (Fig. 6) and Cd–O–Zn (Fig. 6), respectively, that indicates the interfacial region of ZnO and dopants. FTIR spectrum of Pb/ZnO nanoparticles showed narrow stretching vibration bands at $900\text{--}1150\text{ cm}^{-1}$ corresponding to Pb–O–Zn and intensity of stretching bands corresponding to Pb–O–Zn comparatively high that indicates the presence of high Pb in ZnO crystalline structure.

Dynamic light scattering

Particle size of modified ZnO nanoparticles was determined by dynamic light scattering (DLS) particle size analyzer

(Malvern Zetasizer—Nano ZS) with 10 μL minimum volume of sample suspension. The average sizes of Ag/ZnO, Cd/ZnO and Pb/ZnO nanoparticles were observed in the range of 210–350 nm (Fig. 7a), 150–360 nm (Fig. 7b) and 60–165 nm (Fig. 7c), respectively. The size of modified ZnO nanoparticles observed by DLS was also confirmed by XRD as well as SEM characterizations.

BET surface area

The specific surface area and porosity measurement of modified ZnO nanoparticles were analyzed by nitrogen adsorption in a Micromeritics TRIstar 3020 nitrogen absorption apparatus (USA). The corresponding nitrogen adsorption–desorption isotherms and the corresponding BET surface area of modified ZnO nanoparticles can be seen in Fig. 8. The surface morphology of Pb/ZnO nanoparticles showed wide and relatively large volume of porosity (Fig. 8) when compared

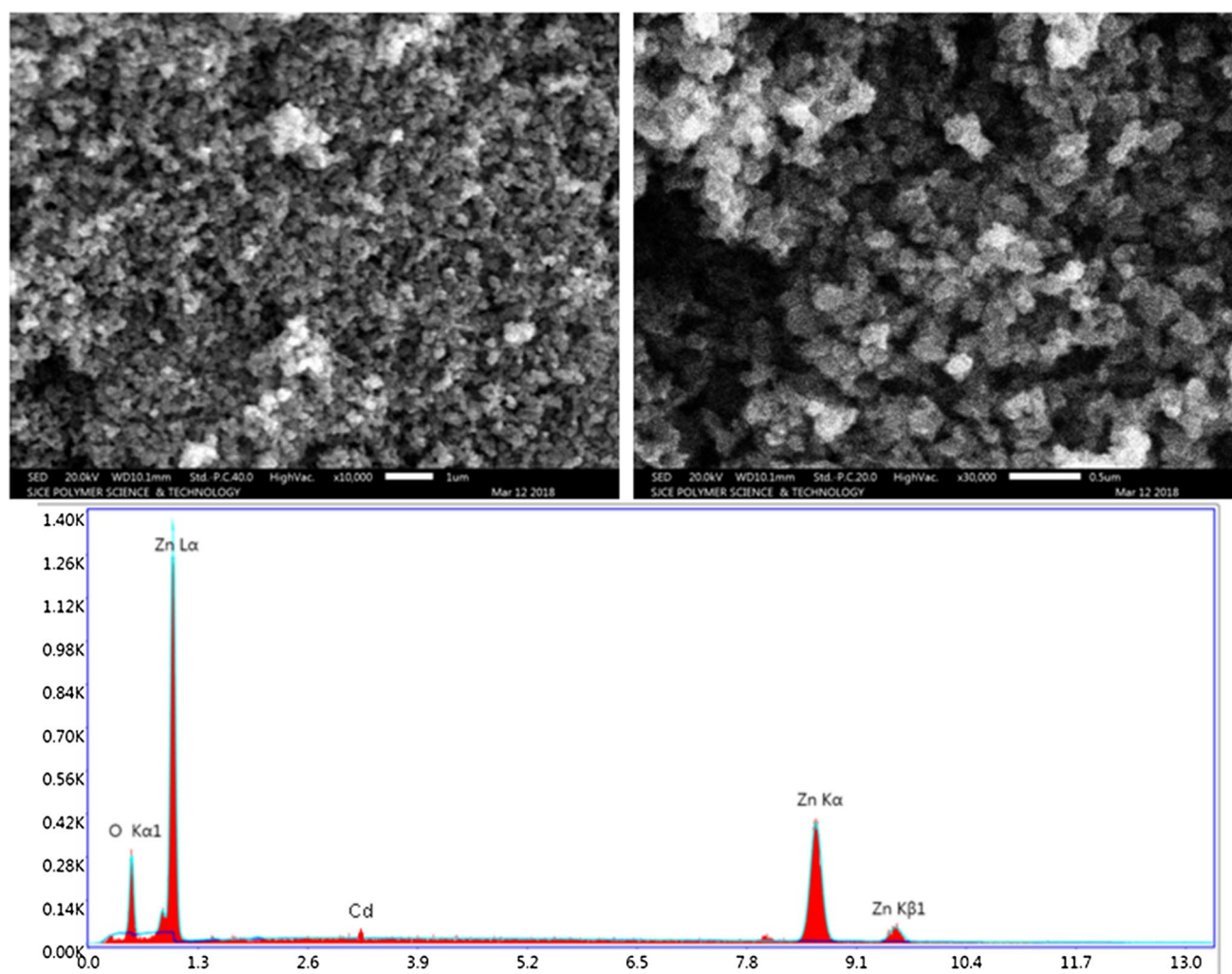


Fig. 4 Scanning electron microscopic images with energy-dispersive X-ray analysis of Cd/ZnO nanoparticles

to Ag/ZnO and Cd/ZnO nanoparticles (Fig. 8a, b). The presence of high amount of nanoporous structures ($0.177176 \text{ cm}^3 \text{ g}^{-1}$) in Pb/ZnO nanoparticles contributed to high pore volume, surface area and pore size. Ag/ZnO and Cd/ZnO showed rough surface morphology and clumping structure with relatively less surface area of 7.75 and $10.6 \text{ m}^2/\text{g}$, respectively, that might be attributed to accumulation of nanoparticles tightly without pore volume, and it was also confirmed by SEM characterization (Figs. 5 and 8c). Pb/ZnO nanoparticles showed considerable increased surface area up to $106.65 \text{ m}^2/\text{g}$, which could be attributed to well-crystalline structure and squared-rod-shaped morphology of nanoparticles.

Photocatalytic activity

Photocatalytic activities of modified ZnO nanoparticles (Ag/ZnO, Cd/ZnO and Pb/ZnO) were studied under

different light sources using aqueous solution of methylene blue dye for 5-h irradiation. The results obtained clearly indicated potential photocatalytic activity of Pb/ZnO nanoparticles under LED light sources than the Ag/ZnO and Cd/ZnO nanoparticles that may be attributed to the well-crystalline and nanorod-shaped morphology observed in Pb/ZnO. All modified ZnO nanoparticles showed considerable photocatalytic degradation efficiency under LED light source followed by tungsten light, but pure ZnO nanoparticles showed potential photocatalytic activity under tungsten light (Fig. 9). The optical studies of modified ZnO nanoparticles also confirmed considerable shifting of band-gap energy toward the visible range that was the possible reason for highest photocatalytic activity under LED (1200 lx) and tungsten light (1600 lx) than UV light source (1000 lx).

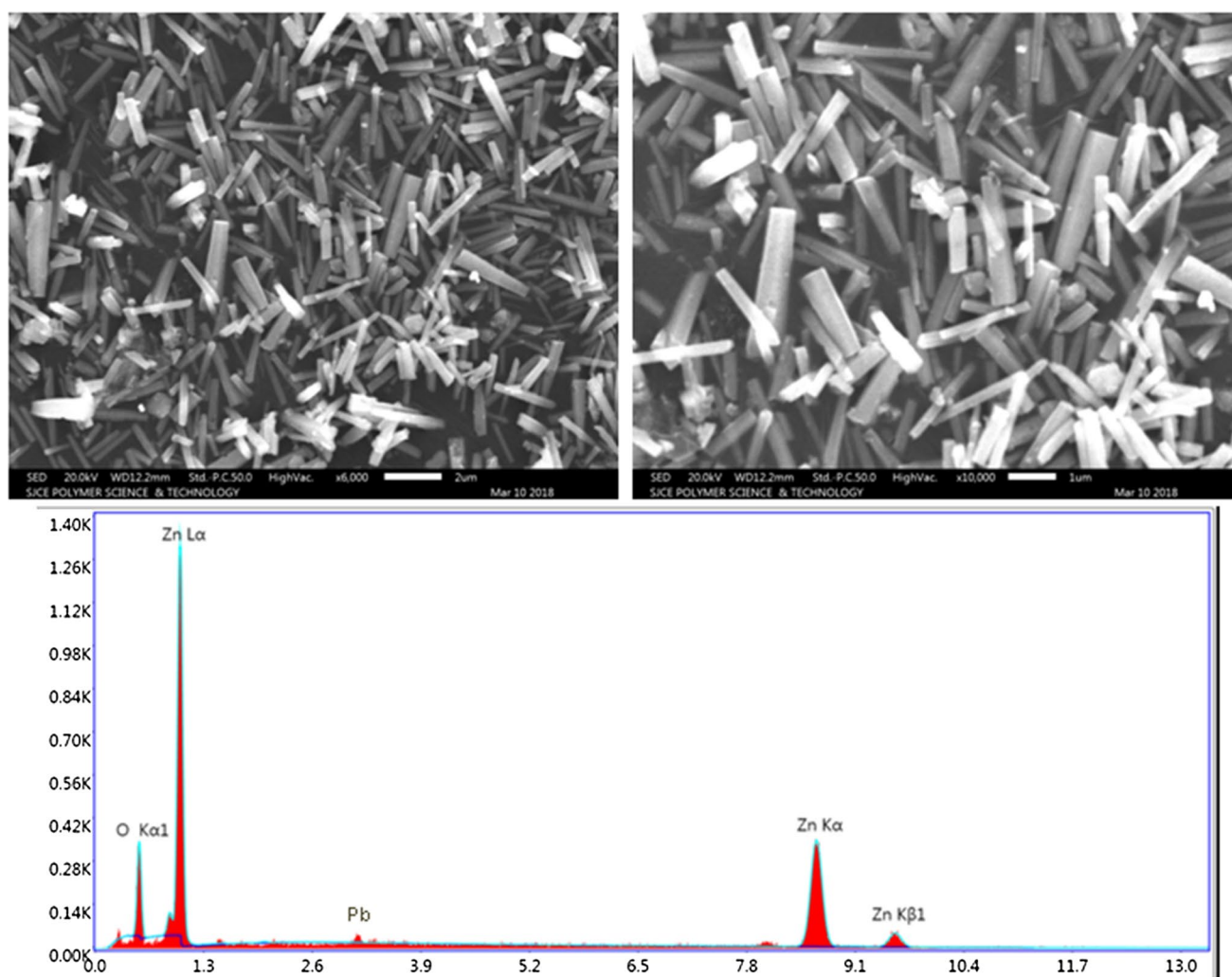
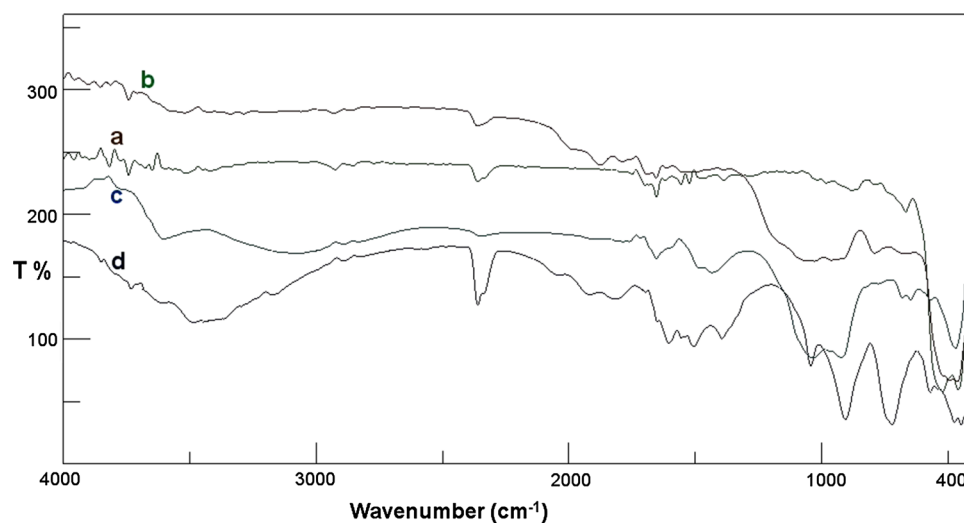


Fig. 5 Scanning electron microscopic images with energy-dispersive X-ray analysis of Pb/ZnO nanoparticles

Fig. 6 FTIR spectra of **a** Pure ZnO nanoparticles; **b** Ag/ZnO nanoparticles; **c** Cd/ZnO nanoparticles; **d** Pb/ZnO nanoparticles



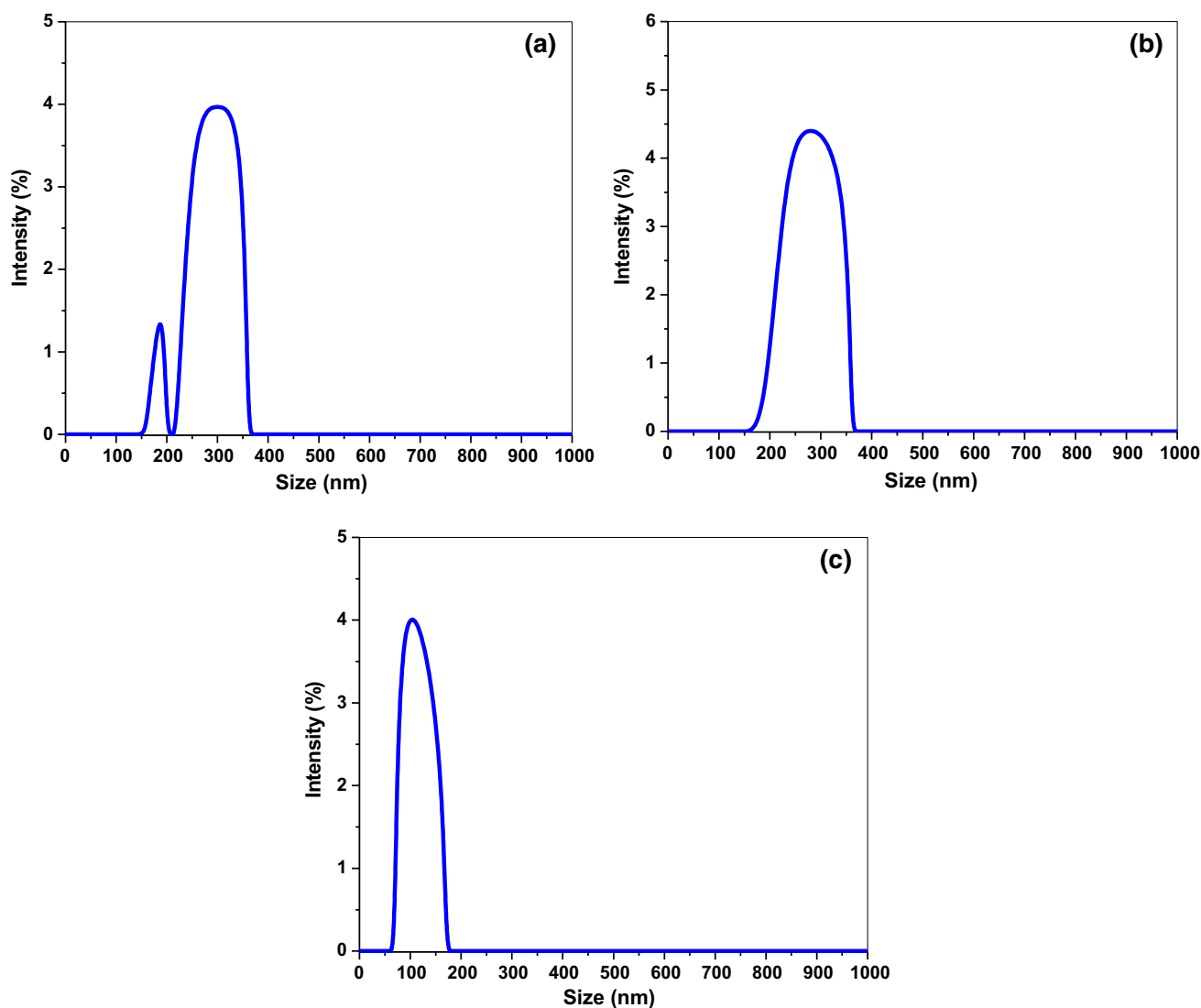


Fig. 7 Dynamic light scattering patterns of **a** Ag/ZnO nanoparticles **b** Cd/ZnO nanoparticles; **c** Pb/ZnO nanoparticles

Degradation of chlorobenzene using modified ZnO nanoparticles

The results obtained clearly indicated that photocatalytic degradation rate of chlorobenzene in an aqueous media using pure ZnO and modified ZnO (Ag/ZnO, Cd/ZnO and Pb/ZnO) nanoparticles found to be highest under tungsten (90%) and LED (96%, 91% and 100%) light sources, respectively. All modified ZnO nanoparticles showed potential degradation efficiency of chlorobenzene in an aqueous media under the visible range that was attributed to considerable band-gap energy shifting toward visible range due to incorporated dopants in ZnO systems. Among the modified ZnO nanoparticles, Pb/ZnO nanoparticles were found to be efficient photocatalyst with rapid degradation rate of chlorobenzene under visible light source (Fig. 10c) and this also

confirmed highest photocatalytic activity in Pb/ZnO nanoparticles. Photocatalytic degradation efficiency of modified ZnO nanoparticles under different light sources can be seen in Fig. 10. Very interestingly, Pb/ZnO nanoparticles showed rapid degradation of chlorobenzene in an aqueous media within short duration (< 120 min) when compared to pure ZnO, Ag/ZnO and Cd/ZnO nanoparticles.

Photocatalytic degradation of chlorobenzene in a vertical continuous photoreactor

Vertical continuous photoreactor model was designed using quartz tube (7 W x 26 cm L) covered with borosil outer shield (10 W x 30 cm L) provided with inlet and outlets. Vertical shaped LED light source was inserted from top of the quartz tube, and upper portion of photoreactor setup was

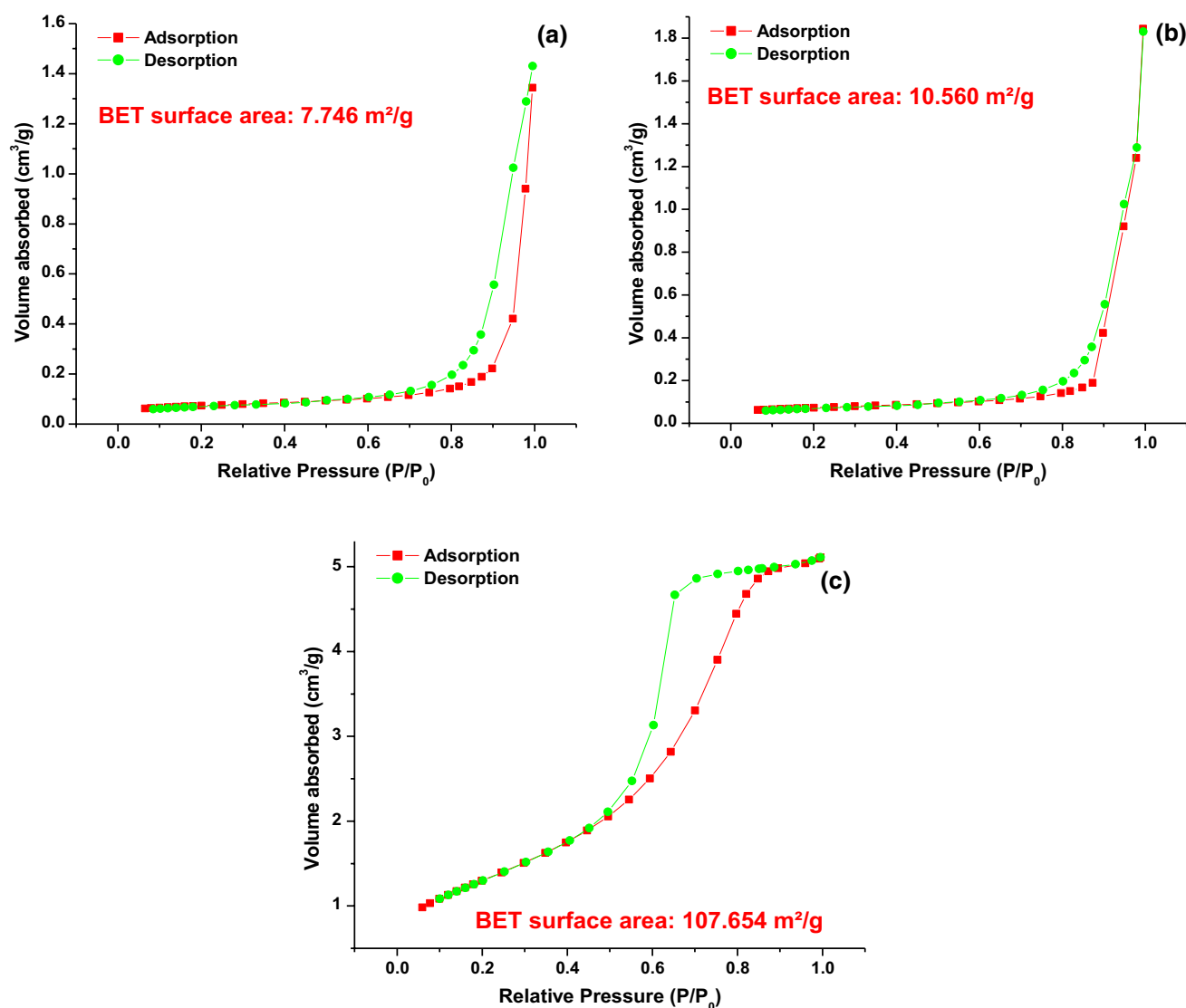


Fig. 8 BET surface area of **a** Ag/ZnO nanoparticles **b** Cd/ZnO nanoparticles; **c** Pb/ZnO nanoparticles

sealed by borosil glass led with air vent and electricity connections. The bottom of borosil outer shield was fixed with stirrer that connected to 16 W external motor for continuous stirring. The outer borosil shield was covered with aluminum sheet to enhance the illumination rate by light reflection, and the vertical continuous photoreactor setup designed can be seen in Fig. 11. The photodegradation efficiency of vertical continuous photoreactor was studied using Pb/ZnO nanoparticles under LED light source by considering important factors such as flow rate, stirring and mode of catalyst load (slurry, floating and immobilize types). The aqueous solution of chlorobenzene (2 L) with 50 µg/L concentration was used for the studies, and external water pump (50 L/h capacity) was used to continuous circulation through the photoreactor. In slurry type of catalyst load, about 1 g of Pb/ZnO nanoparticles was suspended in the aqueous solution and

aqueous mixture was pumped continuously into photoreactor through inlet. In floating type, Pb/ZnO nanoparticles were coated onto 2-mm Teflon beads using standard technique (Kumar et al. 2011) and directly suspended into reaction chamber of the photoreactor. In immobilized type, Pb/ZnO nanoparticles were coated inner surface of outer shield by spreading technique using water proof binding agent (Kumar et al. 2011). All borosil tube (2 cm diameter) connections with reaction vessels were made leak proof with valves and connectors, and flow rate was controlled by pump speed and valves. Photocatalytic degradation efficiency of photoreactor designed using Pb/ZnO nanoparticles was determined by analyzing initial and final concentration of chlorobenzene under GC–MS techniques.

The photodegradation results obtained using continuous-vertical photoreactor setup showed 100% degradation

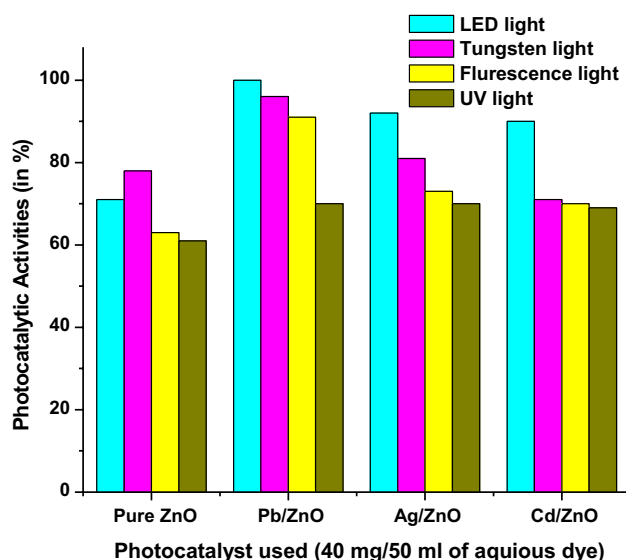


Fig. 9 Photocatalytic activities of modified ZnO nanoparticles under different light sources

rate within 2 h with flow rate of 10 L/h under LED light (Fig. 12a). The results showed highest degradation efficiency in slurry type when compared to floating and immobilized type of catalyst load (Fig. 12b). Potential degradation efficiency in slurry type catalyst load may be attributed to complete and potential exposing of individual catalyst particles to photons and availability of active sites that apparently enhances the production rate of hydroxyl radicals in aqueous media. In floating and immobilized type of catalyst load, catalyst's surface that was adhere and bounded to the substrates (Teflon beads or borosil surface) would not be exposed to light sources or not available for photocatalytic activity in an aqueous media. Effect of stirring on photocatalytic degradation rate in the photoreactor was studied with different speeds and the results obtained indicated that moderate stirring mechanism significantly enhances the

photocatalytic degradation efficiency in slurry type of catalyst load (Fig. 12c). It was also confirmed that degradation rate was also considerably influenced by flow rates (Fig. 12d) that might be attributed to the contact time of catalyst and chlorobenzene in the aqueous media. By considering the photoreactor type, it was confirmed that the irradiation time and flow rates depend on the types of photoreactor models and catalyst to be used. Query ID="Q1" Text="Please check and confirm the section headings are correctly identified."

Conclusions

The solgel preparation of modified ZnO nanoparticles was found to be effective in the degradation of chlorobenzene. The prepared Ag/ZnO, Cd/ZnO and Pb/ZnO have optimized band-gap energy of 2.97, 2.91 and 2.81, respectively. The crystalline size of the nanoparticle which was determined by using XRD is found to be 191.8, 287.7 and 71.9 nm for Ag/ZnO, Cd/ZnO and Pb/ZnO, respectively. SEM image of Ag/ZnO, Cd/ZnO is found to be irregular in shape and aggregated, whereas for Pb/ZnO is truncated nanorod-shaped morphology with well-spaced nanoparticles that appears to be well-crystalline phase. Average particle size and BET surface area of Ag/ZnO, Cd/ZnO and Pb/ZnO nanoparticles are found to be 210–350 nm and 7.456 m²/g, 150–360 nm and 10.56 m²/g and 60–165 nm and 107.654 m²/g, respectively. Modified ZnO nanoparticles are effective in the degradation of chlorobenzene in the visible range spectrum. About 100% of chlorobenzene removal efficiency was obtained for Pb/ZnO nanoparticle within a short duration (< 120 min) under visible light source. To determine the efficiency of the photocatalyst, a vertical continuous reactor model was designed and demonstrated. Highest removal efficiency of chlorobenzene was obtained in a slurry-type reactor when compared to floating and immobilized type. The irradiation time and flow rate are the important factors to be considered for the effective degradation.

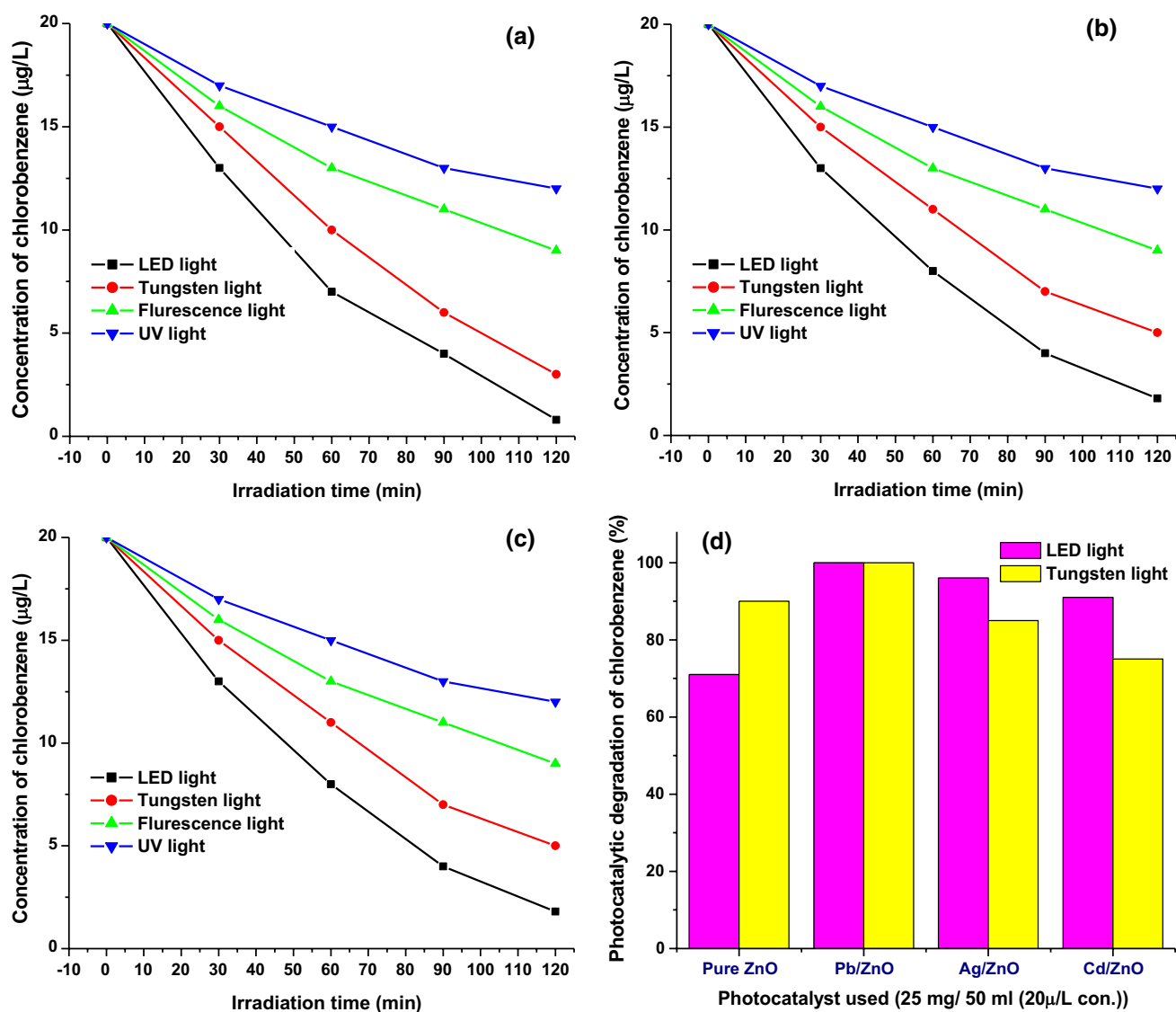
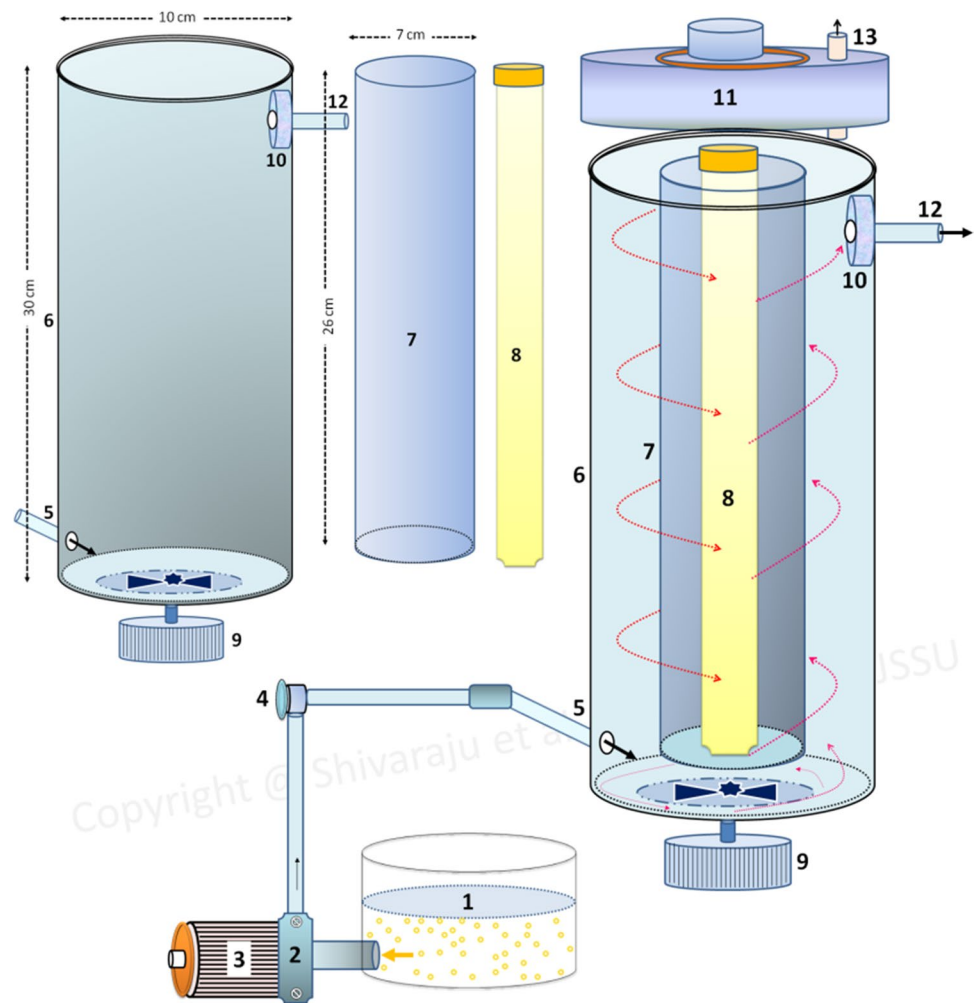


Fig. 10 Photocatalytic degradation of chlorobenzene using **a** Ag/ZnO; **b** Cd/ZnO; **c** Pb/ZnO and **d** Degradation efficiency (in %) of chlorobenzene using pure ZnO and modified ZnO nanoparticles under LED and tungsten light sources

Fig. 11 Continuous photoreactor vertical model: (1) aqueous solution of chlorobenzene (50 $\mu\text{g/L}$) with Fe–Mn–CeO₂/TiO₂ composite nanoparticles; (2) water pump with 50 L/h; (3) motor 320 V; (4) flow controlling valve with glass pipe set (2 cm diameter); (5) inlet of photoreactor; (6) borosil outer shield (10 cm W x 30 cm L); (7) quartz inner cover (7 cm W x 26 cm L); (8) light source (LED bulb, 16 W); (9) stirrer with machine; (10) nanomembrane filter; (11) upper lid with light intensity controller and electric connections; (12) outlet of photoreactor; (13) gas outlet of photoreactor



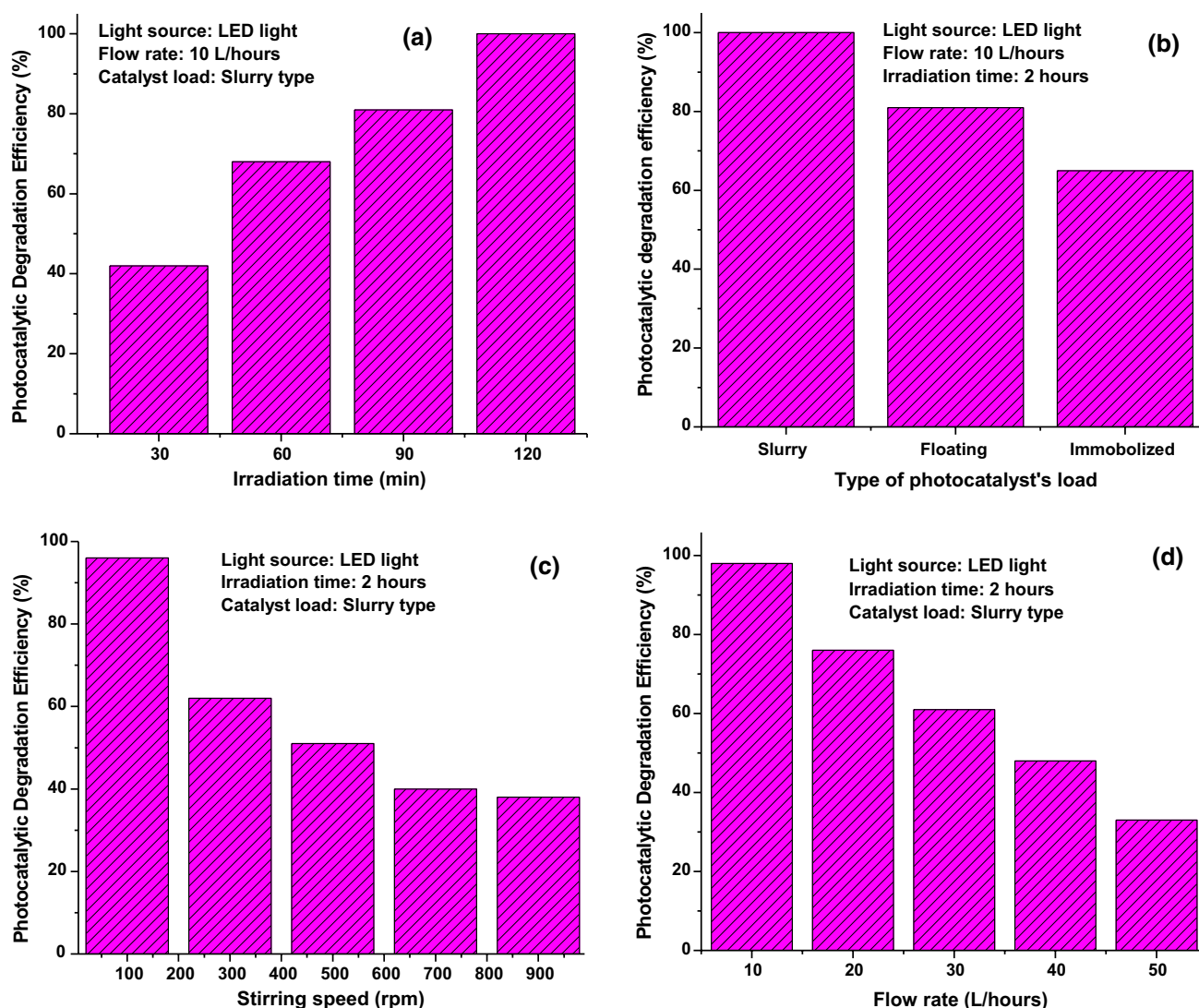


Fig. 12 Photocatalytic degradation of chlorobenzene using continuous (vertical) photoreactor setup **a** effect of irradiation time; **b** effect of photocatalyst's loading type; **c** effect of stirring speed; **d** effect of flow rate

Acknowledgements The authors would like to thank JSS Academy of Higher Education and Research (JSS AHER), Mysuru, India, for providing financial assistance to conduct the research work. University of Mysore and JSS Science and Technology University, Mysuru, acknowledged for instrumentation facilities. The authors thank Dr. Anil Kumar KM, Pallavi S, Midhun G researcher fellows from Department of Water and Health, JSS AHER for providing necessary assistance to complete the research work.

Funding The authors declare that they have no funding supported for this research.

Compliance with ethical standards

Conflict of interest The authors declare that they have no conflict of interest.

Open Access This article is licensed under a Creative Commons Attribution 4.0 International License, which permits use, sharing, adaptation, distribution and reproduction in any medium or format, as long as you give appropriate credit to the original author(s) and the source, provide a link to the Creative Commons licence, and indicate if changes were made. The images or other third party material in this article are included in the article's Creative Commons licence, unless indicated otherwise in a credit line to the material. If material is not included in the article's Creative Commons licence and your intended use is not permitted by statutory regulation or exceeds the permitted use, you will need to obtain permission directly from the copyright holder. To view a copy of this licence, visit <http://creativecommons.org/licenses/by/4.0/>.

References

Ameta R, Benjamin S, Ameta A, Ameta SC (2012) Photocatalytic degradation of organic pollutants: a review. Mater Sci Forum

- 734:247–272. <https://doi.org/10.4028/www.scientific.net/MSF.734.247>
- Anandan S, Ikuma Y, Niwa K (2010) An overview of semi-conductor photocatalysis: modification of TiO_2 nanomaterials. *Solid State Phenom* 162:239–260. <https://doi.org/10.4028/www.scientific.net/SSP.162.239>
- Aneesh PM, Vanaja KAMKJ (2007) Synthesis of ZnO nanoparticles by hydrothermal method. *Nanophotonic Mater IV*. <https://doi.org/10.1117/12.730364>
- Bacaksiz E, Parlak M, Tomakin M, Özçelik A, Karakız M, Altunbaş M (2008) The effect of zinc nitrate, zinc acetate and zinc chloride precursors on investigation of structural and optical properties of ZnO thin films. *J Alloys Compd* 466:447–450. <https://doi.org/10.1016/j.jallcom.2007.11.061>
- Berenjian A, Chan N, Malmiri HJ (2012) Volatile organic compounds removal methods: a review. *Am J Biochem Biotechnol* 8:220–229. <https://doi.org/10.3844/ajbbbsp.2012.220.229>
- Brintha SR, Ajitha M (2015) Synthesis and characterization of ZnO nanoparticles via aqueous solution, sol-gel and hydrothermal methods. *IOSR J Appl Chem* 8:66–72. <https://doi.org/10.9790/5736-081116672>
- Castellote M, Bengtsson N (2011) Applications of titanium dioxide photocatalysis to construction materials. *Springer Int Publ*. <https://doi.org/10.1007/978-94-007-1297-3>
- Chen X, Mao SS (2007) Titanium dioxide nanomaterials: synthesis, properties, modifications and applications. *Chem Rev* 107:2891–2959. <https://doi.org/10.1021/cr0500535>
- Chen YF, Lee CY, Yeng MY, Chiu HT (2003) The effect of calcination temperature on the crystallinity of TiO_2 nanopowders. *J Cryst Growth* 247:363–370. [https://doi.org/10.1016/S0022-0248\(02\)01938-3](https://doi.org/10.1016/S0022-0248(02)01938-3)
- Crutzen PJ, Lawrence MG, Pöschl U (1999) On the background photochemistry of tropospheric ozone. *Tellus. Ser A Dyn Meteorol Oceanogr* 51:123–146. <https://doi.org/10.1034/j.1600-0870.1999.t01-1-00010.x>
- Das D, Gaur V, Verma N (2004) Removal of volatile organic compound by activated carbon fiber. *Carbon N Y* 42:2949–2962. <https://doi.org/10.1016/j.carbon.2004.07.008>
- Djurišić AB, Leung YH, Ching Ng AM (2014) Strategies for improving the efficiency of semiconductor metal oxide photocatalysis. *Mater Horizons* 1:400. <https://doi.org/10.1039/c4mh00031e>
- Eltoumy N (2009) Reduction of anthropogenic volatile and semi-volatile organic compounds by nanomaterials and photolysis. *Molecules* 21:56
- Font X, Artola A, Sánchez A (2011) Detection, composition and treatment of volatile organic compounds from waste treatment plants. *Sensors* 11:4043–4059. <https://doi.org/10.3390/s110404043>
- Goldstein Allen H (2007) Known and Unexplored organic constituents in the earth's atmosphere. *Environ Sci Technol* 41:1514–1521
- Guo H, Kwok NH, Cheng HR, Lee SC, Hung WT, Li YS (2009) Formaldehyde and volatile organic compounds in Hong Kong homes: concentrations and impact factors. *Indoor Air* 19:206–217. <https://doi.org/10.1111/j.1600-0668.2008.00580.x>
- Hasnidawani JN, Azlina HN, Norita H, Bonnia NN, Ratim S, Ali ES (2016) Synthesis of ZnO nanostructures using sol-gel method. *Procedia Chem* 19:211–216. <https://doi.org/10.1016/j.proche.2016.03.095>
- Huang Y, Ho SSH, Niu R, Xu L, Lu Y, Cao J, Lee S (2016) Removal of indoor volatile organic compounds via photocatalytic oxidation: a short review and prospect. *Molecules*. <https://doi.org/10.3390/molecules21010056>
- Khan FI, Ghoshal A (2000) Removal of volatile organic compounds from polluted air. *J Loss Preven Process Ind* 527:545. [https://doi.org/10.1016/S0950-4230\(00\)00007-3](https://doi.org/10.1016/S0950-4230(00)00007-3)
- Khan R, Khan M, Hameedullah AH, Ansari A, Lohani M, Khan R, Ahmad I, Husain FM, Khan W, Alam M (2014) Flower-shaped ZnO nanoparticles synthesized by a novel approach at near-room temperatures with antibacterial and antifungal properties. *Int J Nanomed* 9:853. <https://doi.org/10.2147/IJN.S47351>
- Kim H, Choi W (2007) Effects of surface fluorination of TiO_2 on photocatalytic oxidation of gaseous acetaldehyde. *Appl Catal B Environ* 69:127–132. <https://doi.org/10.1016/j.apcatb.2006.06.011>
- Kumar D, Abhang RM, Taralkar SV (2011) Design of photocatalytic reactor for degradation of phenol in wastewater. *Int J Chem Eng Appl* 2:3144–3148. [https://doi.org/10.1016/S0045-6535\(01\)00327-7](https://doi.org/10.1016/S0045-6535(01)00327-7)
- Lin L, Chai Y, Zhao B, Wei W, He D, He B, Tang Q (2013) Photocatalytic oxidation for degradation of VOCs. *Open J Inorg Chem* 03:14–25. <https://doi.org/10.4236/ojic.2013.31003>
- Malekshahi Byranvand M, Kharat AN, Fatholahi L, Beiranvand ZM (2013) A review on synthesis of nano- TiO_2 via different methods. *JNS* 3:1–9
- Malik A, Hameed S, Siddiqui MJ, Haque MM, Muneer M (2013) Influence of ce doping on the electrical and optical properties of TiO_2 and its photocatalytic activity for the degradation of remazol brilliant blue R. *Int J Photoenergy*. <https://doi.org/10.1155/2013/768348>
- Meena RK, Chouhan N (2015) ZnO nanoparticles synthesized by a novel approach at room temperature and antibacterial activity. *Science* 56:68–72
- Midhun G, Shivaraju HP, Anil Kumar KM (2017) Effects of cationic ligands addition in hydrous titanium oxide on fluoride removal efficiency in aqueous medium. *Int J Environ Health Technol* 1(1):1–7
- Nakata K, Fujishima A (2012) TiO_2 photocatalysis: design and applications. *J Photochem Photobiol C Photochem Rev* 13:169–189. <https://doi.org/10.1016/j.jphotochemrev.2012.06.001>
- Prabhat Kumar T, Anil Kumar M, Chandrajit B (2011) Biofiltration of volatile organic compounds (VOCs)—an overview. *Res J Chem Sci Res J Chem Sci* 1:2231–2606
- Prieto O, Feroso J, Irusta R (2007) Photocatalytic degradation of toluene in air using a fluidized bed photoreactor. *Int J Photoenergy*. <https://doi.org/10.1155/2007/32859>
- Rajput N (2015) Methods of preparation of nanoparticles—a review. *Int J Adv Eng Technol* 7:1806–1811
- Ramesh S (2013) Sol-gel synthesis and characterization nanoparticles $\text{Ag}_3(2+x)\text{Al}_x\text{Ti}_{4-x}\text{O}_{11}+\delta$ ($0.0 \leq x \leq 1.0$). *J Nanosci* 13:9
- Rangkooy H, Rezaee A, Khavanin A, Jafari AJ, Khoopaie A (2012) A study on photocatalytic removal of formaldehyde from air using ZnO nanoparticles immobilized on bone char background and objectives: formaldehyde is one of the toxic polluted air. *Photocatalysis* 7:1–4
- Reddy VL, Kim PKH, Kim YH (2011) A review of photocatalytic treatment for various air pollutants. *Asian J Atmos Environ* 5:181–188. <https://doi.org/10.5572/ajae.2011.5.3.181>
- Rehman S, Ullah R, Butt AM, Gohar ND (2009) Strategies of making TiO_2 and ZnO visible light active. *J Hazard Mater* 170:560–569. <https://doi.org/10.1016/j.jhazmat.2009.05.064>
- Said Ismail OM, Hameed RSA (2013) Environmental effects of volatile organic compounds on ozone layer. *Pelagia. Res Libr Adv Appl Sci Res* 4:264–268
- Salahuddin NA, El-kemary M, Ibrahim EM (2015) Synthesis and characterization of ZnO nanotubes by hydrothermal method. *Int J Sci Res Publ* 5:3–6
- Sharma A, Karn RK, Pandiyan SK (2014) Synthesis of TiO_2 nanoparticles by sol-gel method and their characterization. *J Basic Appl Eng Res* 1:2350–2377
- Shivaraju HP (2012) Hydrothermal synthesis of ZnO nanostructures onto calcium aluminosilicate ceramic supports. *J Nano Sci Nano Technol* 6(1):5–8
- Shivaraju HP, Byrappa K (2012) The role of hydrothermally prepared supported photocatalytic composite in organic micro-pollutants removal from the water. *J Environ Sci Eng* 54(3):353–364

- Shivaraju HP, Chandrashekar CK (2012) Photocatalytic removal of organic pollutants in silk industrial effluents by ZnO deposited CASB supported composite. *Int J Res Chem Environ* 2(2):26–31
- Shivaraju HP, Muzakkira N, Shahmoradi B (2016) Photocatalytic treatment of oil and grease spills in wastewater using coated N-doped TiO₂ polyscales under sunlight as an alternative driving energy. *Int J Environ Sci Technol* 13(9):2293–2302
- Tanizaki T, Murakami Y, Hanada Y, Ishikawa S, Suzuki M, Shinohara R (2007) Titanium dioxide (TiO₂)-assisted photocatalytic degradation of volatile organic compounds at ppb level. *Carbon N Y* 53:514–519
- Tseng TK, Lin YS, Chen YJ, Chu H (2010) A review of photocatalysts prepared by sol-gel method for VOCs removal. *Int J Mol Sci* 11:2336–2361. <https://doi.org/10.3390/ijms11062336>
- Wong CL, Tan YN, Mohamed AR (2011) A review on the formation of titania nanotube photocatalysts by hydrothermal treatment. *J Environ Manag* 92:1669–1680. <https://doi.org/10.1016/J.JENVMAN.2011.03.006>
- Zaleska-medynska A (2006) UV/VIS light enhanced photocatalysis for water treatment and protection. Springer Int Publ. <https://doi.org/10.1007/978-1-4020-4728-2>
- Zou L, Hu E, Luo Y, Atkinson S (2004) Experimental study of the degradation of volatile organic compounds by photocatalytic oxidation using TiO₂ pellets. In: Brebbia (ed) *Air pollution XII C*. WIT Press
- Zou L, Luo Y, Hooper M, Hu E (2006) Removal of VOCs by photocatalysis process using adsorption enhanced TiO₂-SiO₂ catalyst. *Chem Eng Process Process Intens* 45:959–964. <https://doi.org/10.1016/j.cep.2006.01.014>

Publisher's Note Springer Nature remains neutral with regard to jurisdictional claims in published maps and institutional affiliations.